Pergamon

0094-5765(95)00013-5

Acta Astronautica Vol. 35, No. 9–11, pp. 633–642, 1995
Copyright © 1995 Elsevier Science Ltd
Printed in Great Britain. All rights reserved
0094-5765/95 $9.50 + 0.00

ON MAKING USE OF LUNAR AND SOLAR GRAVITY ASSISTS IN LUNAR-A, PLANET-B MISSIONS†

JUNICHIRO KAWAGUCHI, HIROSHI YAMAKAWA, TONO UESUGI and HIROKI MATSUO

Systems Engineering Division, Institute of Space and Astronautical Science, 3-1-1 Yoshinodai, Sagamihara, Kanagawa 229, Japan

(Received 1 July 1994; received for publication 6 February 1995)

Abstract—ISAS (the Institute of Space and Astronautical Science, Japan) is currently planning to launch the LUNAR-A spacecraft to the Moon in 1997 and the PLANET-B spacecraft toward Mars in 1998. Since these two spacecraft have been facing mass budget hurdles, ISAS have been studying how to make good use of lunar and solar gravity effects in order to increase the scientific payload as much as possible. In the LUNAR-A mission, the current orbital sequence uses one lunar swingby via which the spacecraft can be thrown toward the SOI (sphere of influence) boundary for the purpose of acquiring solar gravity assist. This sequence enables the approach velocity to the Moon to be diminished drastically. In the PLANET-B mission, use of lunar and solar gravity assist can help in boosting the increase in velocity and saving the amount of fuel. The sequence discussed here involves two lunar swingbys to accelerate spacecraft enough to exceed the escape velocity. This paper focuses its attention on how such gravity assist trajectories are designed and stresses the significance of such utilization in both missions.

1. INTRODUCTION

The Institute of Space and Astronautical Science (ISAS) is undertaking the launches of spacecraft for space observations and interplanetary explorations by means of the Mu series of launch vehicles. Currently, ISAS is planning to launch the LUNAR-A spacecraft to the Moon in 1997 and the PLANET-B spacecraft toward Mars in 1998 by M-V which is ISAS's new generation Mu series launch vehicle that is under development. With an increase in the scientific payload on those spacecraft, design of M-V has been intensively reexamined so that spacecraft mass is to be commensurate with its mass capability. In spite of these efforts, these two spacecraft have been facing mass budget hurdles. Since they are unmanned scientific spacecraft, flight period and arrival time are not so strongly constrained in comparison with either manned or practical spacecraft. In this context, ISAS has been studying how to make good use of lunar and solar gravity effects in order to cope with such a mass budget austerity.

As for the lunar gravity assists, ISAS launched two spacecraft HITEN[1,2] in 1990 as well as GEOTAIL [3] in 1992, both of which demonstrated double lunar swingby orbits so that geomagnetic tail coverage may have been assured. They took the same trans-lunar sequences which utilized a four and a half revolution scheme that proved quite robust and promising for injection error compensation and launch window expansion. Besides, what HITEN demonstrated in 1992 showed that solar gravity assist around the boundary of the Earth's SOI (sphere of influence) saved fuel around the Moon by reducing the relative velocity to the Moon. These facts so far experienced by ISAS were evidence which future trajectory planning can take advantage of.

The objective of the LUNAR-A mission is further understanding of the origin and evolution of the Moon by means of lunar penetrators[4]. The LUNAR-A spacecraft plants three penetrators on the surface of the Moon so that a seismic and heat-flow measurement network can be built which discloses the interior structure of the Moon by use of a seismometer and heat-flow probe. Seismic data are relayed via a communication orbiter that should be the mother ship carrying the penetrators. Up to one third of spacecraft was directed to fuel amount and saving fuel leads to an increase in the scientific and base system. Also in this lunar orbiter mission, current orbital sequence includes use of one lunar swingby via which spacecraft can be thrown away toward the Earth's SOI boundary for the purpose of acquiring solar gravity assist. This sequence enables the approach velocity to the Moon to be diminished drastically. In the vicinity of the Moon, this approaching velocity is even more reduced via the ballistic capture mechanism which is the product of Earth–Moon interaction [5,6]. This ballistic capture type transfer will be adopted instead of the conventional Hohmann-type transfer

†Paper IAF-93-A.6.46 presented at the *44th International Astronautical Federation Congress*, Graz, Austria, 16–22 October 1993.

in the LUNAR-A mission. The mechanism of solar perturbation for reducing relative velocity with respect to the Moon as well as ballistic capture is investigated, and the design concept for its application to the Earth–Moon transfer is presented here as well.

The PLANET-B is a Mars orbiter mission that aims at plasma physics observation currently under fabrication at the ISAS, whose launch is slated for 1998[7,8]. The PLANET-B spacecraft leaves Earth with a C3† of approximately 10 km^2/s^2. The ISAS is planning to make it fly boosted by means of lunar and solar gravity assists. The sequence discussed here involves two lunar swingbys to accelerate the spacecraft enough to exceed the escape velocity. Historically speaking, a similar attempt was made previously in the case of the ICE spacecraft that was moved from the Sun–Earth libration point L1 toward comet Giacobini–Zinner in 1985[9]. The essence lies in making the spacecraft trajectory retrograde during the first and second lunar swingbys so that the resulting relative velocity to the Moon can be raised. This paper discusses how the multiple lunar gravity assist scheme can be utilized for interplanetary missions taking advantage of the heliocentric gravity affect. The major results here provide a generic and universal design chart, based on which any escape trajectory with multiple lunar gravity assist can be assessed and designed. It summarizes the lead and lag in phase angle as a function of the solar elongation angle, through which appropriate swingby points can be obtained and the initial elongation angle determined. A rigorous baseline trajectory for the PLANET-B spacecraft is represented.

2. LUNAR AND SOLAR GRAVITY EFFECT

Perturbative gravity effects intentionally utilized in the LUNAR-A and PLANET-B missions are investigated and summarized here (except for the well known lunar swingby mechanism).

2.1. Solar effect (Sun–Earth interaction)

The solar gravity effect on Earth orbit is initially investigated which LUNAR-A/PLANET-B makes the most of. Two-body energy as well as angular momentum with the Earth as the central body should remain unchanged if no force other than Earth gravity works on spacecraft motion. Nevertheless, when solar gravity is considered, it causes variation of them. Figure 1 depicts the gravity field due to the Sun where Earth gravity is not taken into account. It is based on the equations of motion derived in an inertial frame (not shown here). It is observed that gravity due to the Sun works outwards near the line connecting the Sun and Earth, which is the product

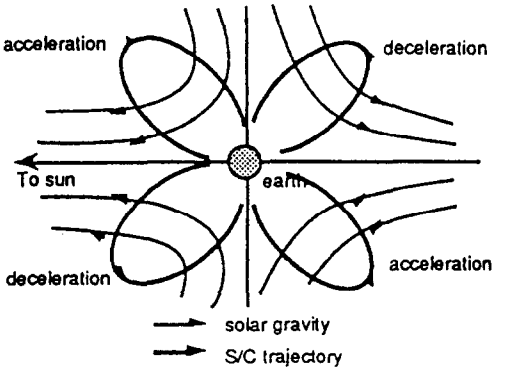

Fig. 1. Solar gravity (Earth gravity not considered).

of the Earth's revolution around the Sun (centrifugal force). Moreover, the following is deduced when a geocentric trajectory is assumed as illustrated in Fig. 1; the spacecraft is more accelerated than in spacecraft–Earth two-body dynamics in the case where it is located in the second or fourth quadrant of the Sun–Earth fixed rotating frame, while in the first and third quadrant the spacecraft is decelerated. Therefore, angular momentum increases when the spacecraft is located in the second or fourth quadrant in the Sun–Earth fixed rotating frame. As to the semi-major axis, this is also enlarged when the spacecraft is located in the second or fourth quadrant in the Sun–Earth fixed rotating frame. Inversely, flight in the first or third quadrant yields a reduction in perigee distance (i.e. angular momentum/semi-major axis) and even reverses the direction of motion into a retrograde one (see[6] for analytical derivation).

2.2. Ballistic capture (Earth–Moon interaction)

The Earth–Moon interaction effect on lunar orbit is investigated in the same manner as solar perturbation. Paying attention to C3 w.r.t. Moon (two-body energy level), it is affected not by the Moon but by the Earth gravity, when the Earth–Moon–spacecraft three-body system is assumed. Figure 2 is a schematic diagram of gravity field due to the Earth in the vicinity of the Moon (without the Moon's effect). Naturally it is observed that, only on the Earth–Moon line, gravity due to the Earth works outward from the Moon in the opposite direction to

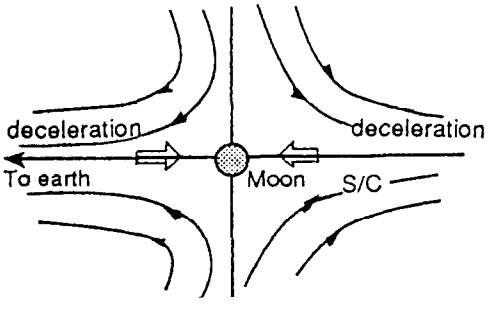

Fig. 2. Gravity field due to the Earth.

†C3 is a two-body energy level in an osculating state (local state) defined in an inertial sense. The relation between the sort of conic section and the sign of C3 is as follows: C3 > 0: hyperbola, C3 = 0: parabola, C3 < 0: ellipse.

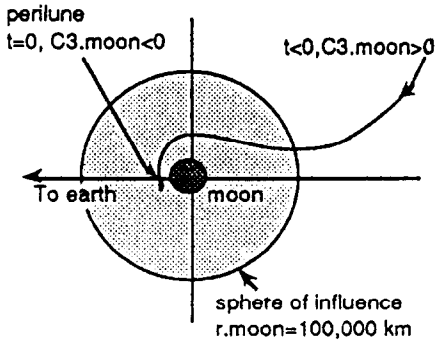

Fig. 3. Definition of ballistic capture.

the Moon's gravity, while on the line perpendicular to the Earth–Moon line, it works towards the Moon. The outward force in the direction of the Earth–Moon line is essentially the product of centrifugal force caused by the Moon's revolution around the Earth. It is this gravity field due to the Earth that influences local lunicentric orbital elements.

Assuming an approaching motion, it is derived that C3 w.r.t. Moon decreases when approaching from the Earth or anti-Earth side in the vicinity of the Earth–Moon line and even becomes negative (see[6] for analytical derivation). This is the principle of ballistic capture, whose definition is as follows: C3 w.r.t. the Moon attains negative value at perilune (i.e. elliptic state), although approaching from the outside (Fig. 3). The approach direction is classified into two subgroups; one from the Earth side, the other from the anti-Earth side. Numerical analysis (not shown here) gives semi-major axis and perigee distance conditions prior to encounter with the Moon, which guarantees ballistic capture at the Moon. When approaching from the Earth side, perigee distance and semi-major axis prior to capture are around 100,000 and 200,000 km, respectively. Minimum perigee distance is around 50,000 km. As to the anti-Earth side approach, perigee distance is around 400,000 km and the semi-major axis ranges from 500,000 km up to several million km prior to ballistic capture. We focus on this kind of trajectory with the anticipation that it may lead to reduction in delta-V for lunar orbit insertion. In astronomy and planetary science, ballistic capture has gained much concern as it has been thought to be one of the candidates which can explain the origin of planetary satellites (see Fig. 4 for example). This type of orbit would be applied for the final portion of LUNAR-A's Earth–Moon transfer trajectory along with the above-mentioned solar perturbative effect on its way to the Moon[5,6].

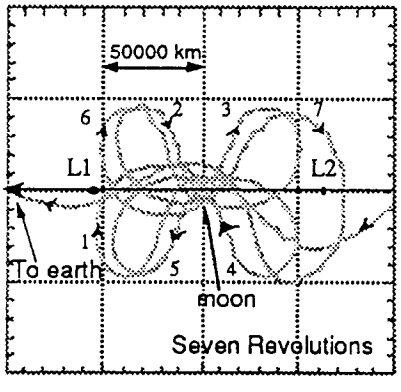

Fig. 4. Example of ballistic capture orbit where an object approaches from outside the Moon and escapes after some revolutions.

3. LUNAR-A MISSION

3.1. How to design an Earth–Moon transfer trajectory with ballistic capture

Earth–Moon transfer followed by ballistic capture is hard to achieve in the Earth–Moon–spacecraft three-body system, since it is difficult to satisfy precapture conditions (i.e. semi-major axis and perigee distance) noted in the previous section if starting from the very near-Earth space. This motivates the effective use of solar gravity. Ballistic capture trajectory approaching the Moon from the Earth side is not appropriate as a short geocentric distance hardly enjoys perturbation by the Sun. On the other hand, ballistic capture from the anti-Earth side through a large geocentric orbit is comparatively suitable because of its liability to solar influence. Therefore, to realize the Earth–Moon transfer trajectory with ballistic capture, solar gravity has to be effectively utilized so that trajectory starts with a low-Earth perigee distance and finally attains a perigee of around Earth–Moon distance with a semi-major axis over 500,000 km. To meet the perigee raise condition, an increase in the local semi-major axis (i.e. C3 w.r.t. Earth) or a decrease in eccentricity is needed. Noting that the Earth–Moon transfer trajectory of our concern lies inside the sphere of influence of the Earth starting from near-Earth space, we cannot expect a drastic change in the semi-major axis under solar influence. Therefore, a decrease in the local eccentricity becomes our main goal. In other words, an increase in angular momentum around the Earth is required for realization of ballistic capture at the Moon.

These observations require the spacecraft to move in the second or fourth quadrant in the Sun–Earth fixed rotating frame to achieve ballistic capture conditions. Taking long duration around the apogee region into account, it may be stated that the apogee positions are to be located in the second or fourth quadrant. This mechanism has two meanings: one is to reach the Moon, the other is to reduce relative velocity w.r.t. Moon. From another point of view, it may be translated that solar gravity works as a substitute for velocity correction at the apogee of the bi-elliptic transfer orbit. The equivalent delta-V at the apogee in a two-body calculation is around 280 m/s.

Trajectory design with ballistic capture is comparatively difficult owing to its high sensitivity to

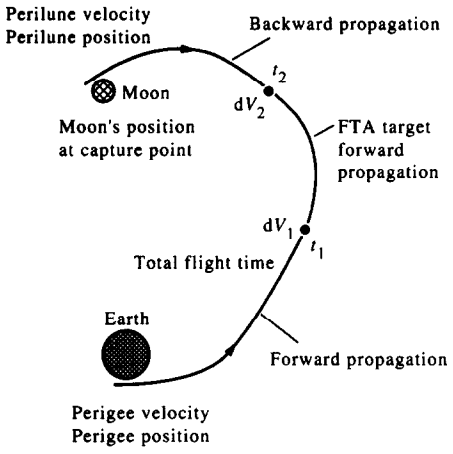

Fig. 5. Earth–Moon transfer trajectory model and control parameters.

initial fluctuation. A trajectory design algorithm is developed whose algorithm is as follows (see Fig. 5):

(a) Earth–Moon transfer trajectory is divided into three segments, by which inherent sensitivity to boundary conditions at Earth departure and lunar insertion is localized and also lowered;
(b) results of analyses concerning ballistic capture (numerical and analytical) as well as solar effect are effectively utilized for the initial guess of the control parameters, i.e. boundary conditions;
(c) midcourse velocity correction is taken into account by use of a fixed time-of-arrival (FTA) target which connects two terminal trajectory segments (corresponding to the inner loop of optimization);
(d) control parameters are optimized by the modified Newton algorithm so that the performance index, constituted of the total velocity correction maneuver, is minimized (outer loop of parameter optimization).

An example of application of this software is shown in Fig. 6 assuming the Sun–Earth–Moon–spacecraft four-body problem, where the orbital profile is plotted in the geocentric Sun–Earth fixed frame and in the Earth–Moon line fixed frame (not regarding the LUNAR-A mission). As to the geocentric portion, thus depicts a single revolution around the Earth in the second quadrant in the Sun–Earth fixed frame. The spacecraft incorporates lunar swingby right after Earth departure and the final approach to the Moon is from the anti-Earth side where C3 w.r.t. Moon is finally negative. This realizes so-called "natural capture" since the spacecraft rotates around the Moon after approaching from outside the Moon's sphere of influence, essentially without the trajectory correction maneuver. These observations are clearly visible when seen in the Earth–Moon fixed frame plots. As a whole, the proposed method shows satisfactory

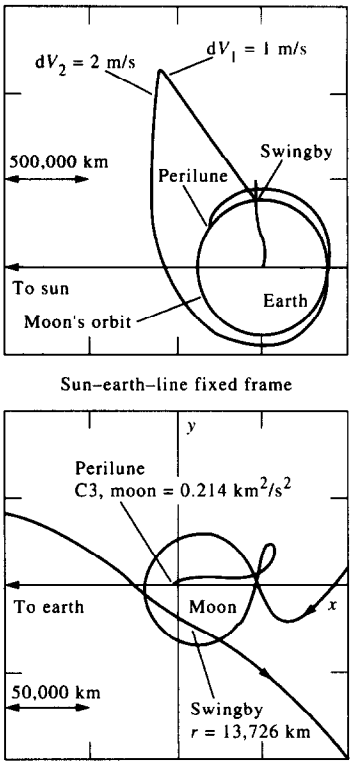

Fig. 6. Orbital profile (four-body problem).

convergence corresponding to initially guessed control parameters through the information of ballistic capture and solar effect analysis. Inversely speaking, the analyses concerning ballistic capture and solar effect on geocentric orbit provide enough information for the design of this kind of trajectory.

3.2. Numerical illustration of orbit synthesis

Figure 7 shows the designed LUNAR-A Earth–Moon transfer trajectory depicted in the geocentric inertial frame whose launch date is in August 1997. ISAS's launch window is especially constrained either in August and September during summer or in January and February for winter. By enlarging the orbit with lunar swingby preceded by the four and a half revolution scheme, the spacecraft arrives at the Moon after a further three and a half month flight. It experiences mainly the fourth quadrant in the Sun–Earth fixed rotating frame (not shown) with a very small amount of fuel expenditure. This enables the spacecraft to take advantage of solar perturbation for the purpose of reducing relative velocity w.r.t. Moon. At lunar orbit, the insertion point at the altitude of 200 km, C3 w.r.t. Moon is negative (i.e. $-0.15\,\mathrm{km^2/s^2}$) by virtue of the ballistic capture mechanism.

Conventional and well-known transfer geometries are Hohmann transfer and bi-elliptic transfer. Bi-parabolic transfer is categorized into an extreme case of bio-elliptic transfer. Hohmann transfer is optimal

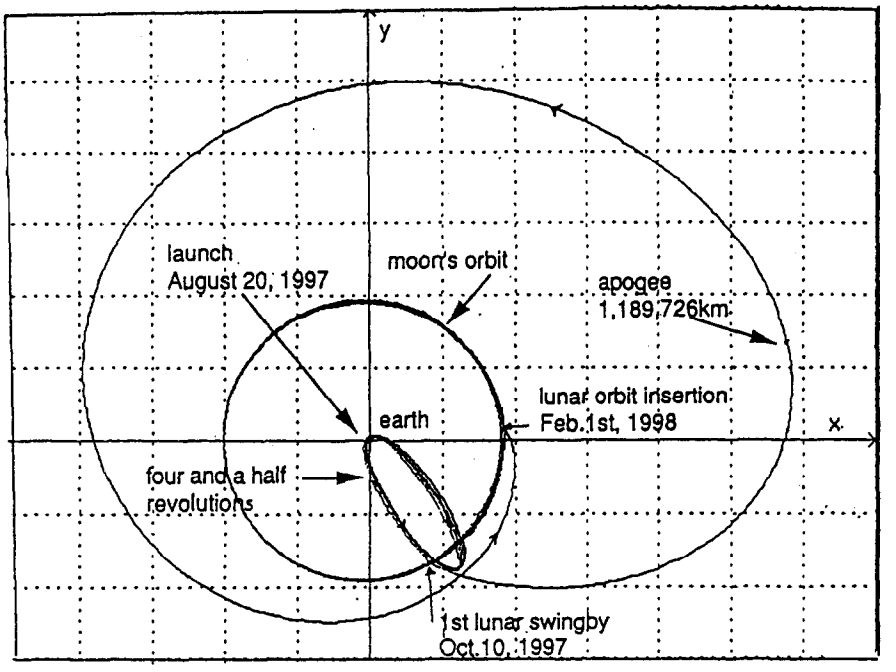

Fig. 7. LUNAR-A orbital profile (geocentric inertial frame).

in the case of transfer from a circular (radius r_1) to circular (radius r_2) trajectory by use of two delta-Vs at terminal points. When the ratio r_2/r_1 is larger than 15.58172, bi-elliptic transfer is superior to Hohmann transfer in terms of total delta-V as long as apogee distance is larger than r_2. When applied to Earth–Moon transfer, r_1 and r_2 take the values of 6578 km (200 km altitude) and 384,400 km respectively, which yields an r_2/r_1 of 58.44. Therefore, bi-elliptic transfer is preferable on the assumption of a circular-to-circular transfer. However, when lunar orbit insertion is taken into account, the result changes drastically. Bi-elliptic transfer becomes equivalent to Hohmann transfer in terms of total delta-V, only when its apogee is as much as 28,200,000 km provided lunar swingby is not used (initial Earth orbit: 200 km-altitude circular orbit, lunar insertion point: 100 km altitude). This states that (without swingby use) bi-elliptic transfer, to say nothing of bi-parabolic transfer, is quite impractical from a flight time point of view when lunar orbit insertion is included in the mission. An interesting point is that, accompanying lunar swingby for orbit enlargement, bi-elliptic transfer becomes superior to Hohmann transfer with reasonable flight time (apogee distance of 1,500,000 km). This is mainly due to the perigee raise effect of swingby, which in turn yields the small required velocity increment at the apogee. Concerning the use of ballistic capture, a flight time of at least three months is needed, while total delta-V is reduced by around 150 m/s in comparison with that of Hohmann-type transfer (see Table 1). If this velocity gain is entirely allotted to the

Table 1 Velocity Gain Allotment in Earth-Moon Transfer with Ballistic Capture
earth departure at 200km altitude circular orbit, lunar insertion at 100km altitude perilune

	Hohmann transfer (PCM*)	bi-elliptic transfer# (PCM*)	ballistic capture type transfer (Num. Int.**)		velocity gain allotment## Hohmann	bi-elliptic
earth injection (m/s)	3,131	3,139	3,144		+13	+5
delta-V at apogee(m/s)	-----	98	3	solar perturbation	+3	-95
lunar orbit	145	15	-47	ballistic capture	-192	-62
total delta-V(m/s)	3,276	3,252	3,100		-176	-152

\# apogee distance =1,500,000 km assuming lunar swingby for orbit enlargement
in comparison with Hohmann and bi-elliptic transfer
* Patched Conic Method
** numerical integration in sun-earth-moon-spacecraft four-body system (see Fig.6)
% delta-V required for insertion into osculating parabolic orbit (C3 w.r.t. moon=0)

reaction control system with a specific impulse (I_{sp}) of 180 s (300 s), then 10% (6%) of the total spacecraft weight can be saved. These results show that Earth–Moon transfer trajectory with ballistic capture is practical from a delta-V and flight time point of view.

4. PLANET-B MISSION

4.1. How to design an escape trajectory via lunar gravity assist

The design strategy of PLANET-B's escape trajectory is discussed next. It is quite obvious that even if multiple lunar swingbys are introduced under two-body approximation, relative velocity to the Moon is invariant. Maximum orbital energy that is obtained by that scheme is limited up to 2 km^2/s^2, which is far below that required in the transfer to Mars which needs 8–9 km^2/s^2. The most fundamental concept that should be stressed here is either to alter the orbit after swingby or to make the spacecraft fly inversely so that the resulting relative velocity to the Moon can be raised (opposite to the LUNAR-A case). The answer to the question is clear and spells out the use of the solar gravity effect without any expenditure of fuel. This method was actually used in the past by ICE (International Comet Explorer) [9] which demonstrated the orbital energy boosted via the solar gravity field. The same approach is also taken here, while the discussion here proposes a design chart applicable to any interplanetary missions with a robust trans-lunar flight scheme.

Figure 8 shows a rotating co-ordinate system in the Sun–Earth line fixed frame. As discussed before, this co-ordinate frame is divided into two major distinct portions, dependent on which solar gravity effect can retrograde spacecraft orbit around the Earth. In the case where the spacecraft makes a swingby in quadrants I and III, the solar gravity effect enables the spacecraft to retrograde, while it directs and lingers starting from quadrant II and IV.

Suppose the longitude of the first swingby point in the inertial frame (ecliptic) is θ_0, that of the Sun direction at the same instance is ϕ_i, and the longitude of the first swingby point in the Sun–Earth line is Φ. These relate to each other as follows:

$$\phi_i + \Phi - 180^\circ = \theta_0,$$

$$\phi_{esc} = FT + \phi_i = FT + \theta_0 - \Phi + 180^\circ, \qquad (1)$$

where ϕ_{esc} denotes the longitude of the Sun direction at the second swingby which is very close to the escape time even if the second swingby takes an extra flight. FT above indicates the flight time measured in days and is approximately an angle between the first and second swingbys centered at the Sun, as a revolution of angular velocity is almost one degree per day as for Earth. Let the longitude advance (lead) angle during the flight between the first and second swingbys be $\Delta\theta$, the longitude of escape direction θ_{esc} is expressed as

$$\theta_{esc}\theta_0 + \Delta\theta + \alpha = \phi_{esc} - \beta. \qquad (2)$$

Here α stands for the phase in the longitude at escape from the second-swingby point, and β indicates the escape direction in the Sun–Earth line fixed co-ordinate. Essentially β is not fixed in the Sun–Earth line fixed frame but should be specified in the inertial frame. However, if discussion is concentrated on a narrow launch window, it can be regarded as frozen even in the Sun–Earth line fixed co-ordinate, which eases the discussion here.

In the use of multiple lunar swingbys, there are a few distinct flight modes; they are denoted here by 2SB−, 2SB+ and 3SB. It should be noted that the spacecraft has to propel at perigee passage as a trans-Mars trajectory requires a C3 of 8–9 km^2/s^2 which is far beyond the scheme with only lunar gravity assist. Since energy sensitivity to orbital maneuver is much more efficient and higher at the perigee than that at the perilune, the burn maneuver will be made when the spacecraft passes the perigee. Consequently, the trajectory after the second swingby never directly connects the interplanetary path but has to pass the low altitude region around the Earth again. Provided

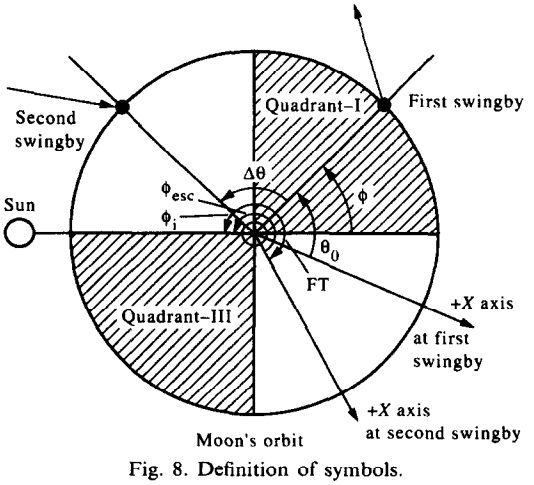

Fig. 8. Definition of symbols.

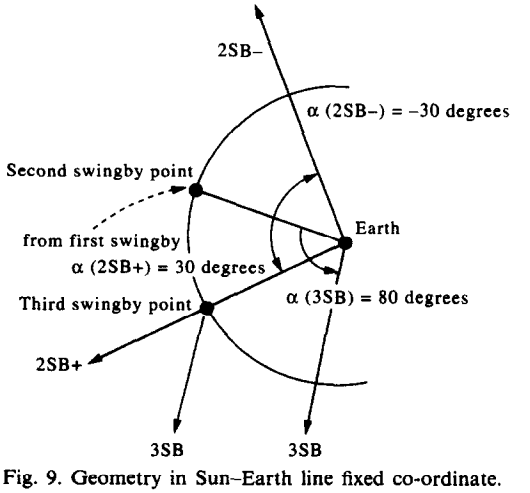

Fig. 9. Geometry in Sun–Earth line fixed co-ordinate.

double lunar swingbys are assumed, even though the trajectory around the Earth retrogrades prior to the second swingby, dependent on whether it also retrogrades to pass the perigee or not, two different paths exist 2SB− and 2SB+, whose schematic drawings are shown in Fig. 9. In 2SB−, the escape direction leads in longitude with respect to the second swingby point, while it loses longitude in 2SB+. Note that 2SB+ corresponds to a higher energy with large deflection at the second swingby. 3SB assumes another swingby boost even after the second swingby, between which the kick maneuver at the perigee is required (Fig. 9). As for the escape energy of 8–9 km^2/s^2, the α angle is around the figures of

$$\alpha = \left\{ \begin{array}{l} 80^\circ \text{ for 3SB} \\ +30^\circ \text{ for 2SB+} \\ -30^\circ \text{ for 2SB−} \end{array} \right\}$$

$$\beta = 60^\circ \text{ for trans-Mars@December 1998.} \quad (3)$$

Here the β angle above holds only if departure from Earth in December of 1998 to Mars is assumed. In other cases, the α figure can be left unchanged, while β is tailored for each window. The discussion here is applicable for other missions such as the transfer to Venus (except the β figure).

The basic idea here is to eliminate θ_0 so that phase-free analysis may be applied. The result is

$$\Delta\theta - \mathrm{FT} + \Phi = \left\{ \begin{array}{l} 40^\circ(-140^\circ)\text{3SB} \\ 90^\circ(-90^\circ)\text{2SB+} \\ 150^\circ(-30^\circ)\text{2SB−} \end{array} \right\} \quad (4)$$

Note that the left-hand-side is a function of only Φ, and that the right-hand-side is governed only by β under the energy band of 8–9 km^2/s^2. The relation above does not contain any variable that depends on ephemeris and can be used as a universal reference. Since the launch from Earth is assumed here, the relative velocity to the Moon at the first swingby is almost frozen to 1 km/s, in general. On the condition that the second swingby must take place synchronously with the Moon's revolution, the trajectory between the first and second swingbys is automatically discretely determined dependent on each Φ in the sense of a restricted three-body problem. Rigorously speaking, they are multifolded comprised of several modes 0 to 3, which stand for the number of the Moon's revolution, during the flight from the first to second swingby. Figure 10(a)–(d) shows the typical plot corresponding to the three modes, where the first swingby point is intentionally set toward the $+x$-axis (phase = 0°), while Φ is found so that the second swingby is met. Through similar numerical simulations, the longitude advance (lead) angle $\Delta\theta$ is obtained together with flight time. Results are summarized in Fig. 11 in which the left-hand-side of eqn (4) as well as flight time, is plotted against the Φ angle. The right-hand-side of eqn (4) is also indicated specifically for Mars transfer in 1998. Note again that this drawing is universal. Suppose a certain suitable departure

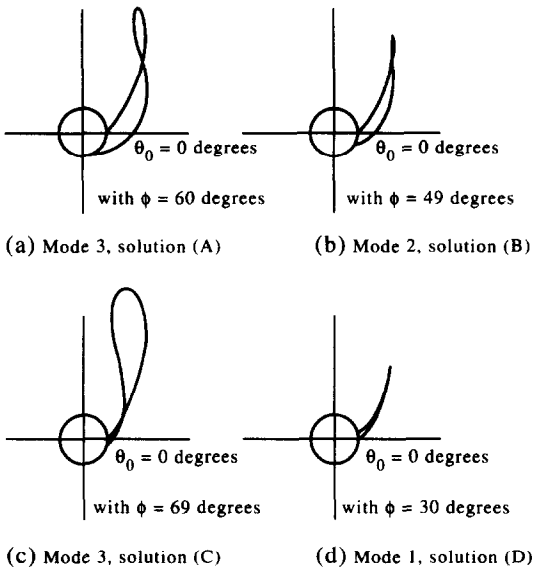

(a) Mode 3, solution (A) (b) Mode 2, solution (B)

(c) Mode 3, solution (C) (d) Mode 1, solution (D)

Fig. 10. Typical trajectories between first and second swingbys.

date from Earth is found with the right ascension angle of escape asymptote, β angle is calculated at once and reference lines such as 2SB−, 2SB+, 3SB are drawn. Intersections of those with solid lines in Fig. 11 give the appropriate initial elongation angle Φ, dependent on which launch date is calculated via flight time denoted by broken lines. In this example

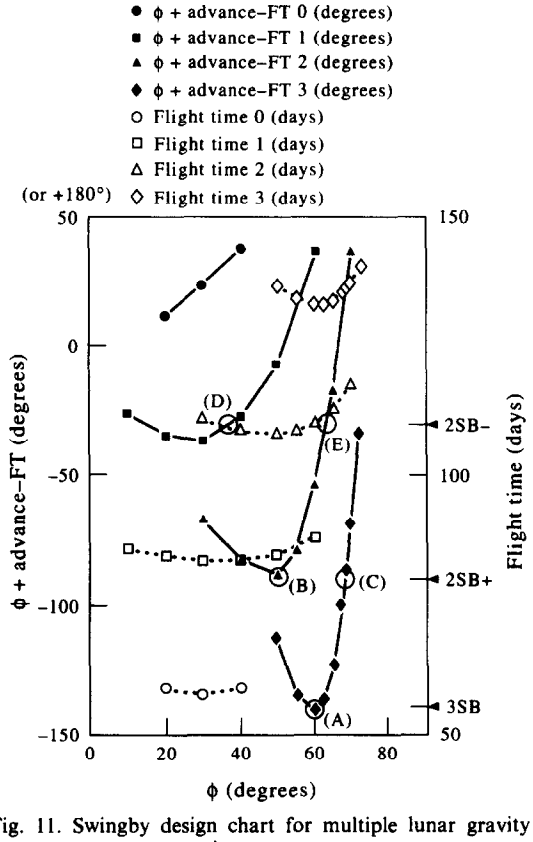

Fig. 11. Swingby design chart for multiple lunar gravity assist to escape.

for Mars transfer in 1998, five solutions are noted which are labeled (A) to (E). It might also be noted here that a steep slope of a solid line is indicative of a high sensitivity to the first swingby point, and a slope of the first swingby should be flat so that orbital synthesis can be eased. Trajectory design comprised of multiple swingbys with the final escape condition is quite hard, since even the slightest initial fluctuation may affect it drastically.

4.2. Numerical illustration of orbit synthesis

In this case, based on another software, an escape date was found around December 1998, whose corresponding β angle was calculated at around 60°. According to Fig. 11, provided solution (A) is taken, the initial Φ is estimated at about 60° or 240°. Besides, flight time is also suggested from Fig. 11 to be 135 days ($4\frac{1}{2}$ months) and the first swingby date is derived as the end of July to beginning of August 1998. In order that three successive lunar swingbys can be made, both semi-major axis (a) and eccentricity (e) associated with the hyperbola between second and third swingbys have to satisfy strict relations. However, since energy sensitivity requests that the final kick burn be made at the perigee and that it should be as low as possible, there is another relation between a and e that might be incompatible with the first requirement. As a result, a and e are governed only by the perigee passage altitude. In other words, final kick burn velocity cannot be arbitrarily specified on the condition that two successive swingbys can be accomplished. The orbit of this type was actually designed with fortunate coincidence, in which the ultimate escape velocity is matched with that prescribed (but not shown here with figures). Usually, the 3SB mode is relatively unflexible. In the case where escape energy is smaller, a 3SB transfer scheme is possible without any extra burn where C3 attained amounts up to 4.2 km^2/s^2 (they are not examples concerning Mars transfer in 1998).

As noted above, solutions (C) and (E) in Fig. 11 are too sensitive to be synthesized. Talking about flight period to escape, solution (A) requires four and a half months, (B) needs three and a half months, while (D) is synthesized within two and a half months. A shorter parking (waiting) period is generally preferable. Although details are not described here, through the ISAS's experiences in the Double Lunar Swingby Demonstrator HITEN and GEOTAIL, a four and a half revolution translunar scheme is well established and found to be feasible for the successful first lunar swingby, since it is much less sensitive to injection errors and is robust. That translunar phase takes about 40–50 days prior to the first swingby and a launch date is requested in August and September, an admissible first swingby opportunity is uniquely determined no earlier than September. This constraint states solution (D) is the only choice ISAS can take.

Figures 12–14 show the designed trajectory (D). What is to be emphasized here is that the trajectory between the first and second swingbys is located in the third quadrant of the Sun–Earth fixed frame and is highly inclined with respect to the Moon's orbital plane against anticipation. This is probably due to the fact that the ecliptic plane does not coincide with the Moon's orbital plane. Notwithstanding, out of plane motion is almost 30 degrees inclined and to be noted.

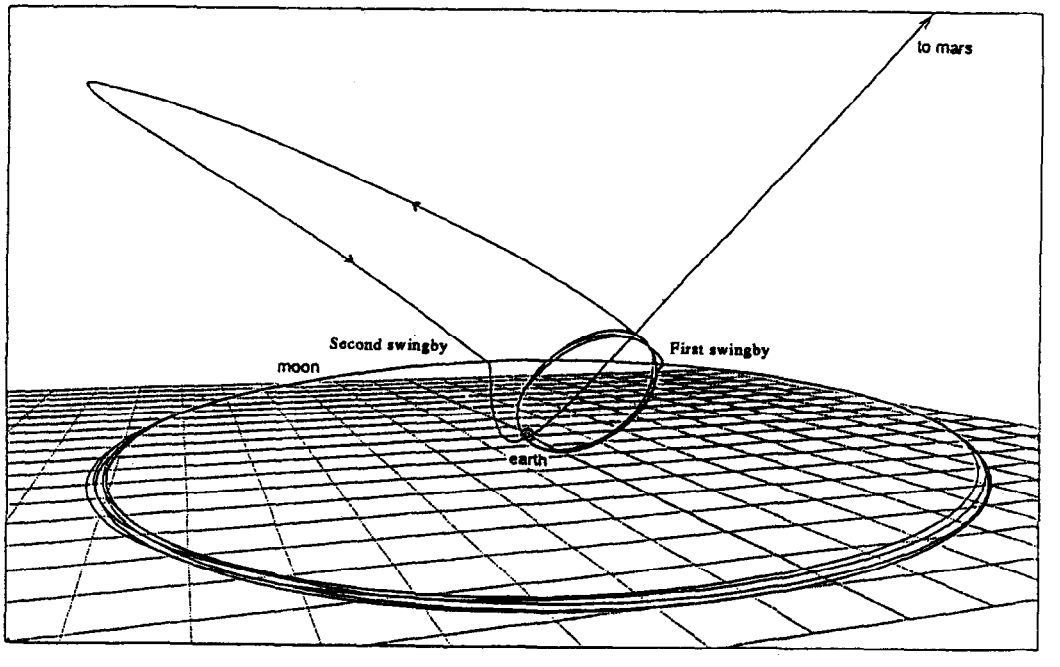

Fig. 12. Trajectory prospect of PLANET-B 1998 (geocentric inertial frame).

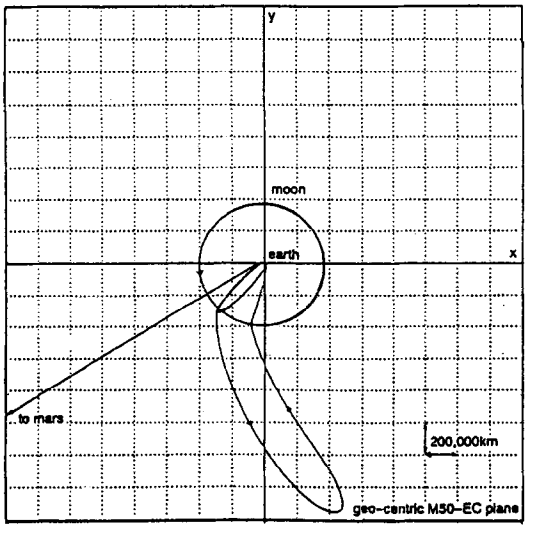

Fig. 13. Rigorous orbit plan of PLANET-B 1998 (geocentric inertial frame).

The second lunar swingby plays a double key role not only in adjusting perigee altitude so that the correct escape ascension can be matched, but in adjusting the decline of the outgoing asymptote, both of which are controlled via targeting phase angle on B-plane defined at the second swingby. Here is another requirement on perigee altitude, which should be as low as possible from an efficiency point of view. However, as noted there are two distinct parameters to be controlled, the correct ascension and the decline of the escape direction, whose degree of freedom is identical to targeting variables at swingby, swingby distance and phase angle on B-plane. Thus perigee altitude is not a parameter that can be directly controlled. What is difficult in utilizing multiple swingbys in an escape mission lies at this point.

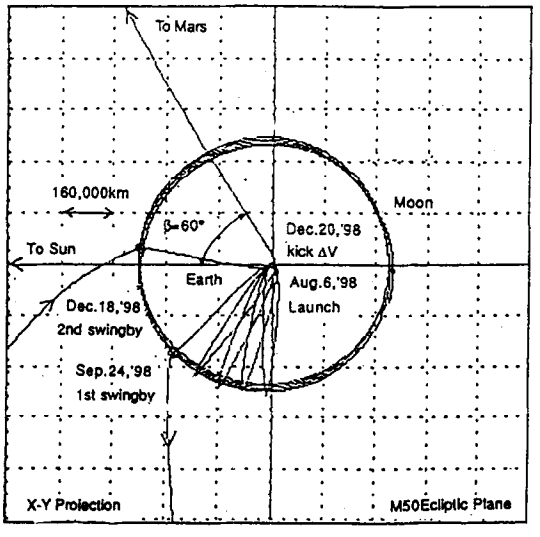

Fig. 14. Rigorous orbit plan of PLANET-B 1998 (Sun–Earth line fixed co-ordinate).

Swingby parameters at the first swingby are exhausted to meet the second swingby. Therefore even if an entire trajectory is found that satisfies the physical equations of motion, a certain optimization is still left to raise maneuver efficiency. Results given in Figs 12–14 were obtained through that optimization process. C3 with Earth as central body after the second swingby is around 1.0 km^2/s^2, having been raised over the escape velocity. The required delta-V applied at the perigee passage is approx. 400 m/s to boost spacecraft the energy of 9.5 km^2/s^2 in C3. Through these acrobatic swingby maneuvers, total delta-V, after the spacecraft is injected onto a higher elliptic orbit (translunar orbit), is reduced by almost 100 m/s, which is converted to a C3 reduction of 2.0 km^2/s^2.

An example, a triple swingby trajectory accelerates the orbital energy from a C3 of -2 to 4 km^2/s^2 within a short leading period (launch to escape) of 6 months. Although this plan accelerates the spacecraft so efficiently, double swingby strategy is found to be more feasible. This is because guidance accuracy at the third swingby is subject to navigation and orbital maneuver errors at the last perigee passage, where boosting is made rather than perilune from an energetic sensitivity point of view. Besides, a shorter stay in this pre-escape phase is preferable. Moreover, the current plan is represented which enables spacecraft to be boosted from a C3 of -2 to 1 km^2/s^2 within four and a half months.

5. CONCLUDING REMARKS

As to the LUNAR-A mission slated for 1997, an orbit design strategy has been discussed which utilizes lunar ballistic capture. When a spacecraft approaches the Moon along this type of trajectory, fuel consumption for velocity reduction at orbit insertion would be reduced by the greatest possible extent, since low relative velocity is attained at its encounter. This in turn yields an increase in the payload for scientific observation. When the Earth–Moon transfer trajectory is considered, a positive use of the solar gravity realizes a path from the vicinity of the Earth to the Moon via ballistic capture, since it works as an effective perturbative force for diminishing relative velocity w.r.t. Moon. The expected gain in C3 w.r.t. Moon over conventional Hohmann-type transfer is 0.8 km^2/s^2, which corresponds to saving of 5–9% of spacecraft mass assuming a specific impulse of 300–180 s. The ballistic capture mechanism was analytically investigated and a systematic procedure for its application to Earth–Moon transfer was established along with solar effect analysis. It was shown that the analyses concerning ballistic capture and solar perturbation provide enough information for design of this kind of trajectory.

Also for the PLANET-B mission, orbit design synthesis has been discussed so far, by making use of multiple swingbys applied to interplanetary escape

missions. The baseline scenario of the PLANET-B mission for the window in 1998 is currently assuming the 2SB+ mode transfer discussed. Although a similar try was once attempted in an ICE mission, what this paper focuses its attention on is rather to establish a universal design diagram (or figure) that is free from any ephemeris, that is practically postulating departure from low-Earth orbit. It was shown that triple lunar gravity assist enables spacecraft to obtain a C3 of 4.5 km^2/s^2 without any use of a propulsive maneuver. The discussion here revealed three potential solutions for PLANET-B in 1998, excluding high sensitive solutions to the first swingby point, for which synthesis can hardly be feasible. Among the three solutions, this paper picked path (D) as a baseline, since the flight period preceding escape is relatively short and compatible with the launch window constraint imposed on ISAS, even though a well-established four and a half revolution transfer to the first swingby is introduced. This practical orbit sequence can be applied to any interplanetary mission, whose lead time (preceding period) is four and a half months including translunar phase. Expected gain in velocity increment is around 2.0 km^2/s^2 converted in C3 w.r.t. Earth, if a type (D) path is used.

REFERENCES

1. K. Uesugi, Space odyssey of an angel—summary of the HITEN's three years mission. *AAS/GSFC International Symposium on Space Flight Dynamics*, paper AAS-93-292, NASA GSFC, 26–30 April (1993).
2. K. Uesugi, J. Kawaguchi, N. Ishii, M. Shuto, H. Yamakawa, and K. Tanaka, Follow-on mission description of HITEN. *Proceedings of the 18th International Symposium on Space Technology and Science*, Kagoshima, pp. 1723–1728, 17–23 May (1992).
3. K. Uesugi, J. Kawaguchi, N. Ishii, H. Yamakawa, H. Terada and M. Matsuoka, GEOTAIL launch window expansion and trajectory correction strategies: analysis and flight results. *5th International Space Conference of Pacific-Basin Societies (ISCOPS)*, Shanghai, China, 6–9 June (1993).
4. H. Mizutani, M. Kohno, S. Tsukamoto, J. Kawaguchi, H. Hinada and K. Ninomiya, Lunar interior exploration by lunar penetrator mission. *41st IAF Congress*, paper IAF-90-039, Dresden, Germany, 6–12 October (1990).
5. E. A. Belbruno and J. K. Miller, Sun-perturbed Earth-to-Moon transfers with ballistic capture. *J. Guid. Control Dynam.* **16**, 770–775 (1993).
6. H. Yamakawa, J. Kawaguchi, N. Ishii and H Matsuo, On Earth–Moon transfer trajectory with gravitational capture. *AAS/AIAA Astrodynamics Conference*, paper AAS-93-633, Victoria, B.C., Canada, 16–19 August (1993).
7. J. Kawaguchi, K. Tsuruda, T. Mukai and I. Nakatani, A Mars mission in space plasma physics. *42nd IAF Congress*, paper IAF-91-466, Montreal, Canada, 5–11 October (1991).
8. J. Kawaguchi, M. Kimura, H. Yamakawa, T. Uesugi, H. Matsuo and R. Farquhar, PLANET-B's lunar gravity assist trajectory to Mars. *AAS/AIAA Astrodynamics Conference*, paper AAS-93-687, Victoria, B.C., Canada, 16–19 August (1993).
9. R. W. Farquhar, D. W. Dunham and S. C. Hsu, Orbital acrobatics in the Sun–Earth–Moon system. *Proceedings of the Second International Symposium on Spacecraft Flight Dynamics*, Darmstadt, Germany, 20–23 October (1986).